Influence of the liquid helium meniscus on neutron reflectometry data

C. J. Kinane[1], O. Kirichek[1], T. R. Charlton[1], P. V. E. McClintock[2]

[1]ISIS Facility, Rutherford-Appleton Laboratory, Chilton, Didcot, United Kingdom

[2]Physics Department, Lancaster University, Lancaster, United Kingdom

Neutron reflectometry offers a unique opportunity for the direct observation of nano-stratification in ^{3}He-^{4}He mixtures in the ultra-low temperature limit. Unfortunately the results of recent experiments could not be well-modelled on account of a seemingly anomalous variation of reflectivity with momentum transfer. We now hypothesize that this effect is attributable to an optical distortion caused by the liquid's meniscus near the container wall. The validity of this idea is tested and confirmed through a subsidiary experiment on a D_2O sample, showing that the meniscus can significantly distort results if the beam size in the horizontal plane is comparable with, or bigger than, the diameter of the container. The meniscus problem can be eliminated if the beam size is substantially smaller than the diameter of the container, such that reflection takes place only from the flat region of the liquid surface thus excluding the meniscus tails. Practical measures for minimising the meniscus distortion effect are discussed.

Introduction

Neutron Reflectometry (NR) has proved to be a powerful tool for studying nano-layers and buried interfaces, especially in view of its suitability for use with a bulky sample environment. This is because neutrons are very penetrating when compared to x-rays, so that they can pass through aluminium vessel walls up to ~ 1 mm thick, without noticeable degradation of the incident beam intensity. Neutrons also have a scattering power, known as the scattering length (b) that varies quasi-randomly across the periodic table, in contrast to x-rays which vary as Z^4, where Z is the proton number [1]. This means that different isotopes of the same element can have very different scattering factors. In the case of ^{4}He the coherent scattering length is 3.26 fm, with no incoherent scattering or significant neutron absorption. For ^{3}He, on the other hand, the situation is significantly different with a coherent scattering factor of 5.74-1.483i fm, where the imaginary number represents a resonant absorption term; it also has a significant incoherent scattering factor of -2.5+2.568i fm that leads to a neutron scattering background.

The information that is obtained by using neutron reflectivity is called the Scattering Length Density profile (SLD) an example of which is shown in fig 2 b) . SLD is the product of the scattering factor b (fm) and the atomic number density N (atoms/Å^3) and is quoted in units of x10^{-6} Å^{-2}, this is usually shown as a function of depth down into the surface that is being reflected off. Hence both the atomic composition and its density are measured. The SLD profile is obtained by iteratively fitting a reflectivity model to the measured reflection data and allows quantities such as surface roughness, thickness and SLD to be ascertained.

Thanks to the nm wavelength often used in neutron reflectivity, this method is particularly efficient in investigating layers of different atoms (multilayers) with almost atomic-plane precision and

distinct physical properties [2,3], or in modelling biological nano-membranes [4] especially for light elements in the periodic table.

More than four decades ago NR was used for the first time at low temperatures (at 1.23 K) for measuring the real part of the bound-atom coherent neutron scattering length of ^{3}He by comparing the reflectivities of quartz-liquid-^{3}He and quartz-liquid-^{4}He interfaces. This parameter was found to have the value $(6.1\pm0.6) \times 10^{-13}$ cm [5]. Much later the reflection of neutrons was observed for the first time from the free surface of liquid ^{4}He [6]. These experiments showed that the ^{4}He surface is smoother in the superfluid state at 1.54 K than in the case of the normal liquid at 2.3 K. In the superfluid state a ~ 200 Å thick surface layer was found that has a subtly different neutron scattering cross-section, which may be explained by an enhanced Bose–Einstein condensate fraction close to the helium surface. In later experiments with neutron reflection from the free surfaces of commercially pure ^{4}He and of a ^{3}He-^{4}He mixture with a ^{3}He concentration of 0.5 % it was found that the addition of ^{3}He isotopic impurities could be leading to the formation of Andreev levels [7] at low temperatures (around 0.3 K) resulting in the formation of a diffusive ^{3}He nano-layer with a thickness of a few hundred Å on the bulk ^{4}He liquid surface [8, 9]. Unfortunately, useful numerical analysis of the experimental data turned out to be impossible. We hypothesise that this unexpected effect was due to an optical distortion caused by deviations from flatness of the liquid surface and, in particular, its meniscus at the wall of the container. In what follows, we test this idea. We describe an investigation of the influence of a meniscus on liquid reflectometry data and we will propose measures minimise the resultant optical distortion effect in reflectometry experiments with the liquid helium isotopes. The results are also applicable to reflectometry from liquids more generally, wherever there is the possibility of a meniscus.

Optical distortion of liquid helium surface

Andreev predicted theoretically [7] that, for dilute ^{3}He in ^{4}He mixtures at zero temperature, ^{3}He atoms will congregate in Andreev states at the surface, forming a 2D Fermi gas. He proposed that these states consist of ^{3}He quasi-particles bound to the liquid surface. The surface effective mass M of a ^{3}He quasi-particle differs from the bulk effective mass, which should result in a 2D layer of Fermi particles, in this case ^{3}He atoms. This picture is only applicable for less than one ^{3}He monolayer. If the density of ^{3}He atoms is such that there are enough atoms to form more than one monolayer then the adsorbed layer of ^{3}He may behave like a 2D Fermi liquid not very different from pure bulk ^{3}He. This picture is based on the results of surface tension experiments [10, 11], surface electron mobility data [12, 13], and a theoretical model [11]. A direct experimental observation of an atomically thin, single, abrupt ^{3}He layer on the surface of a dilute ^{3}He/^{4}He mixture has not yet been achieved, and no information is available about the distribution of ^{3}He near the helium surface as a function of depth. If it were possible to create and control such an experimental system, it would provide an almost ideal model for studying 2D/3D Fermi liquid surface excitations [14, 15] and it could be used in the search for a superfluid transition in 2D ^{3}He on the surface of nano-separated ^{3}He/^{4}He liquid mixtures [16]. Neutron reflectometry offers a unique opportunity for direct observation of nano-stratification/interdiffusion of the ^{3}He/^{4}He mixture in the ultra-low temperature limit.

In our initial experiments on neutron reflection from liquid helium surfaces [6, 8, 9] at the ISIS neutron scattering facility, we used the general-purpose time-of-flight (TOF) polarised reflectometer

CRISP [17]; in later experiments we used the next-generation reflectometer POLREF [18]. The experimental set-up used for the liquid helium experiments is described in [6].

We thus investigated the surface properties of liquid ^{3}He/^{4}He mixtures by neutron reflection for temperatures in the range 0.08 < T < 2.2 K [8, 9], both for commercial helium with ~ 0.3 ppm (3x10^{-5} %) of ^{3}He, and for a stronger 0.1 % ^{3}He/^{4}He mixture. We also collected neutron reflection data from very high purity ^{4}He with ~ 3 ppb of ^{3}He (3x10^{-7} %) [21], which gave us the opportunity of studying the ideal case of almost pure ^{4}He.

Data were collected as a function of intensity normalized to an incident beam measurement *vs.* angle. One fixed angle was used on each beamline for the wavelength ranges 0.5 Å to 6.5 Å on CRISP and 1 Å to 12 Å on POLREF, respectively, using the TOF method. Note that this was not monochromatic scattering. The momentum transfer Q_z is inversely proportional to the neutron wavelength λ:

$$Q_z = \frac{4\pi}{\lambda} \sin \theta$$

where θ is the fixed angle of incidence in TOF operation.

Fig. 1 shows reflectivity curves collected from the surface of high purity liquid ^{4}He at different temperatures: the results for 2.3 K, 1.5 K and 0.4 K are almost identical within their error bars (Fig. 1a). In the case of a 0.1 % of ^{3}He in ^{4}He mixture, however, the situation is completely different (Fig. 1b). At 2.3 K the reflectivity curve coincides with the pure ^{4}He case because the ^{3}He is effectively diluted and does not scatter strongly, but when the temperature is decreased to 1.5 K the reflectivity curve deviates from the high temperature one. At 0.4 K the difference is even larger, most likely due to the formation of a significant diffuse layer of ^{3}He near the surface. This layer would scatter much more strongly than bulk ^{4}He, whence the increase in the reflectivity, but it would also generate more incoherent scattering, thereby increasing the neutron background. These experimental results allow us to infer the formation of denser ^{3}He layer, probably consisting of occupied Andreev states near the surface of the bulk liquid. However we failed to fit a quantitative neutron reflection model to the data, so that we could not evaluate specific parameters of the diffuse layer for comparison with the corresponding theoretical values. The main obstacle to data fitting is an unexpected "bump" that can be observed on all curves for Q_z around 0.01 Å^{-1}, which is not predicted by the standard reflectometry model (solid blue line in Fig. 2 a).

In Fig 2 a) we show data for isotopically purified ^{4}He, fitted with the NR model described in [19, 20] with the GenX x-ray and neutron reflectivity fitting package [23]. This data agrees exceptionally well with the model, having a figure of merit χ^2 = 1.4. A χ^2 of 1 is considered a perfect fit. The SLD profile is also good replication of that shown in Ref [6] as in this paper we have refitted the original data set with the new fitting package to check the validity of the initial model. For the scientific implications of the SLD profile we again direct you to Ref [6]. It should be noted at this point that the density of liquid ^{4}He changes with temperature and has to be taken into account in the initial calculation of the He isotope SLD. The experimental data [22] used to seed the fits is displayed in Fig 2 c). An essential difference between the two experiments displayed in Figures 1 and 2, was that the horizontal dimension (beam footprint) of the neutron beam in the high purity ^{4}He experiment was only 70 % of the cell's inner diameter (31.4 mm) whereas, in the new experiment, the beam dimension was

several times that of the cell diameter. We suggest that it was this increase in beam dimension relative to the cell that was responsible for the "bump" in Fig. 1 a), because it would have brought the meniscus of the liquid helium, i.e. a surface of variable height, into the beam.
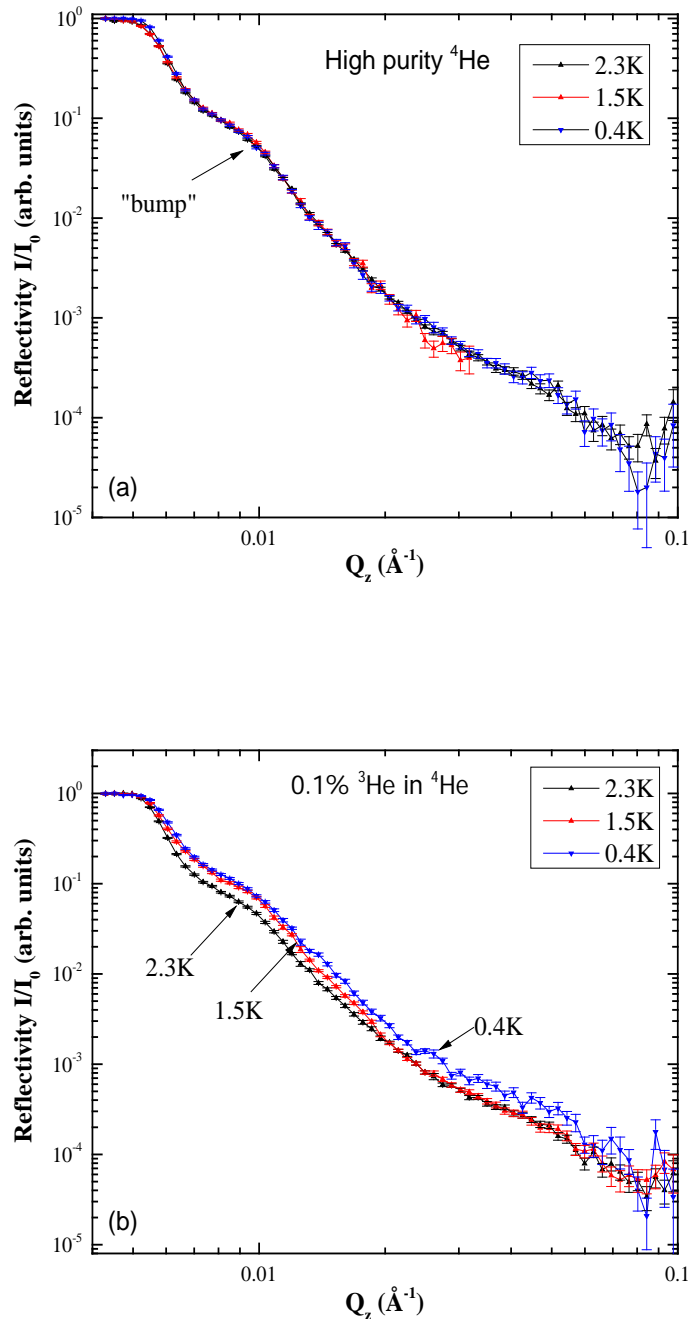

Fig. 1 Surface reflectivity curves collected at different temperatures: 2.3 K, 1.5 K and 0.4 K from (a) isotopically purified helium; and (b) 0.1 % ^{3}He/^{4}He mixture. We hypothesise that the seemingly anomalous "bump" indicated by the arrow in Fig. 1a) is attributable to optical distortion caused by the liquid helium meniscus.

Having a beam footprint significantly smaller than the diameter of the cell in the old experiment would have minimized distortion due to the meniscus, but it also made the data collection time much longer (on the order of several days rather than hours). Our new experiment, with a beam dimension comparable with the diameter of the cell facilitated much faster data collection, adequate for completion within the beam-time allocated for this experiment – but would have suffered from the putative distortion effect. It is worth mentioning that in the new experiment we used a ^{3}He evaporation refrigerator Heliox VL®. This meant an additional two layers of aluminum from refrigerator's vacuum can windows with a combined thickness of ~ 1 mm, as compared to the old measurement cryostat. This additional aluminum in the beam slightly increased the background signal and beam degradation, and made measurements take slightly longer, but was corrected for in the direct incident beam measurement used to normalize the reflectivity.
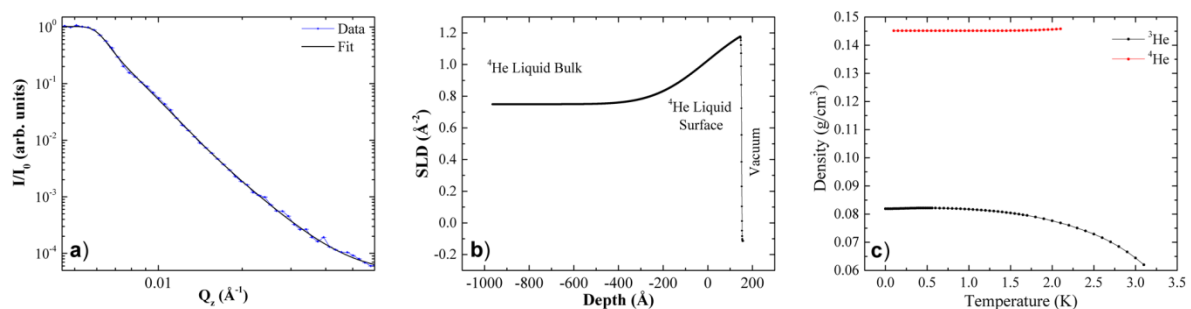

Fig. 2: a) High purity ^{4}He NR curve with fit, taken with a beam foot print 70 % the size of the sample can diameter. b) SLD profile used to generate the NR fit in the first panel. c) Low temperature liquid density's for ^{3}He and ^{4}He Isotopes.

Model tests with liquid D_2O surface.

To test the hypothesis, a more trackable system was required in order to quantify the effects of the meniscus *vs.* the size of the beam footprint. Heavy water (D_2O) was chosen because it produces high intensity neutron reflection due to the large scattering factor of deuterium (6.671 fm). This allows relatively quick measurements, with high contrast, using an area detector. The area detector is often referred to as a 1D detector, where the time of flight generates a second dimension for the area maps. As can be seen in Fig. 3, if the beam dimension in the horizontal plane is approximately 50% smaller than the diameter of a 65mm container half-filled with liquid D_2O, no distortion can be observed. However if the beam dimension in the horizontal plane is comparable (90%) with the container diameter of 34 mm (as in the new cell used for the helium experiments) there is significant optical distortion due to the meniscus (Fig. 4). The periodic pattern in the reflection signal may be attributed to the interference of neutron waves on a curved surface [24]. This further illuminates the difference between the pure ^{4}He and mixed isotope data sets.
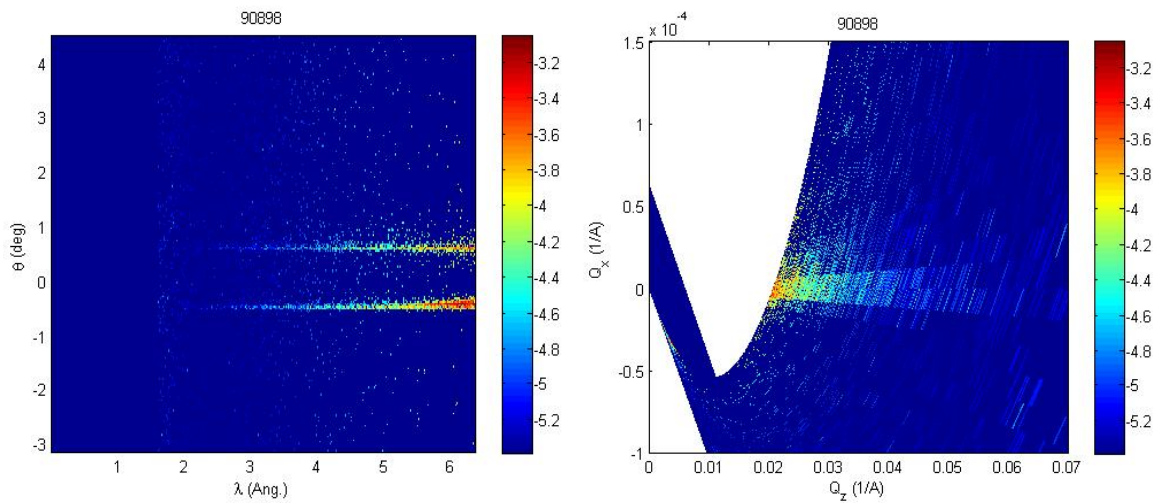
Fig. 3 Reflectivity signal maps shown on an area detector from a D$_2$O surface in a sample cell of 65 mm diameter. The neutron beam's horizontal dimension is significantly smaller than cell's diameter. There is no distortion due to the effect of the meniscus.
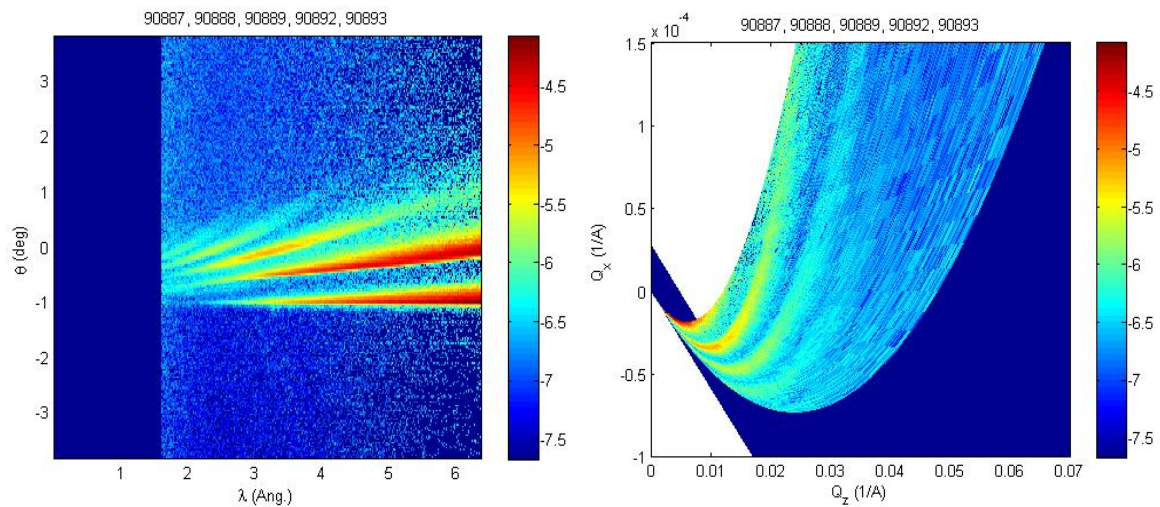

Fig. 4 Reflectivity signal maps shown on an area detector from a D$_2$O surface in a sample cell of 35 mm diameter. The neutron beam's horizontal dimension is comparable with the cell diameter. We can see a periodic pattern in the reflection signal that can be explained by the interference of neutron waves on a curved surface.

Conclusion

We have attributed seemingly anomalous neutron reflectivity data from liquid helium to the influence of the meniscus at the container wall. We have shown that the meniscus can significantly distort the reflectometry data if the beam size in the horizontal refection plane (beam footprint) is comparable with the diameter of the container. We have also confirmed that the effect is

negated/reduced if the beam size is significantly less than the diameter of the container such that it largely avoids interacting with the surface of the curved meniscus. The most practical way of avoiding meniscus distortion effects would be to increase the dimensions of the liquid container such that the beam footprint reflects off the largest, flattest, area possible, far from the region of the meniscus. However, this inevitably carries implications for the effective construction and operation of a sub-Kelvin cryostat system due to the increase in heat load. We would recommend using a rectangular vessel, where possible, to maximise the useable surface area in the container, given that a circular geometry does not utilise optimally the square beams used on most reflectometers. We plan to implement both of these changes in our further experiments utilizing neutron reflectometry to study nano-layered ^{3}He formed at the surface of weak ^{3}He/^{4}He mixtures at ultra-low temperatures.

Acknowledgements

1. G.A.D. Ritchie and D. S. Sivia, *Foundations of Physics for Chemists*, Oxford University Press (2000).
2. L.J. Collins-McIntyre, S.E. Harrison, P. Schönherr, N. Steinke, C.J Kinane, *et al.*, *Europhys. Lett.* **107,** 57009 (2014).
3. J. Reguera, E. Ponomarev, T. Geue, F. Stellacci, F. Bresme, *et al.*, *Nanoscale* **7**, 5665 (2015).
4. R. Budvytyte, M. Mickevicius, D.J. Vanderah, F. Heinrich, and G. Valincius, *Langmuir* **29**, 4320 (2013).
5. T.A. Kitchens, T. Oversluizen, L. Passell, and R.I. Schermer, *Phys. Rev. Lett.* **32**, 791 (1974).
6. T. R. Charlton, R. M. Dalgliesh, O. Kirichek, S. Langridge, A. Ganshin, and P. V. E. McClintock, *Low Temp. Phys.* **34,** 316 (2008).
7. A.F. Andreev *Zh. Exp. Teor. Fiz.* **50**, 1415 (1966).
8. T. R. Charlton, R. M. Dalgliesh, A. Ganshin, O. Kirichek, S. Langridge, and P. V. E. McClintock, *J. Phys.: Conf. Series* **150,** 032022 (2009).
9. O. Kirichek, N. D. Vasilev, T. R. Charlton, C. J. Kinane, R. M. Dalgliesh, A. Ganshin, S. Langridge, and P. V. E. McClintock, *J. Phys.: Conf. Series* **400,** 012033 (2012).
10. H. M. Guo, D. O. Edwards, R. E. Sarwinski, and J. T. Tough, *Phys. Rev. Lett.* **27**, 1259 (1971).
11. D.O. Edwards and W.F. Saam, *Prog. Low Temp. Phys.* **VII A**, ed. D. F. Brewer, North Holland, Amsterdam, 1978, p. 283.
12. B.N. Esel'son, A.S. Rybalko, and S.S. Sokolov, *Sov. J. Low Temp. Phys.* **6**, 544 (1980).
13. H. Yayama and Y. Yatsuyama, *J. Low Temp. Phys.* **175**, 401 (2014).
14. S.S. Sokolov, J.-P. Rino, and N. Studart , *Phys. Rev. B* **55**, 14473 (1997).
15. Kirichek, M. Saitoh, K. Kono, and F.I.B. Williams, *Phys. Rev. Lett.* **86**, 4064 (2001).
16. H.N. Robkoff, D.A. Ewen, and R.B. Hallock, *Phys. Rev. Lett.* **43**, 2006 (1979).
17. R. Felici, J. Penfold, R. C. Ward, and W. G. Williams, *Appl. Phys. A: Solids Surf.* **45**, 169 (1988).
18. http://www.isis.stfc.ac.uk/instruments/polref/
19. L.G. Parratt, *Phys. Rev.* **95,** 359 (1954).
20. S.J. Blundell and J.A.C. Bland, *Phys. Rev. B* **46,** 3391 (1992).
21. R.J. Scott and P.V.E. McClintock, *Phys. Lett. A* **64,** 205 (1977).

22. B.N. Esel'son, V.N. Grigor'ev, V. G. Ivantsov, E.Ya. Rudavskii, D.G. Sanikidze, I.A. Serbin. Solutions of the quantum liquids HeS-He4 (in Russian) Moscow, Nauka (1973).

23. M. Björck and G. Andersson J. Appl. Cryst. 40, 1174 (2007)

24. R. Pynn, SPIE: Neutron Optical Devices and Applications, 1738, 270 (1992).